



# HHS Public Access

Author manuscript

*J Biomed Mater Res B Appl Biomater.* Author manuscript; available in PMC 2020 February 01.

Published in final edited form as:

*J Biomed Mater Res B Appl Biomater.* 2019 February ; 107(2): 314–323. doi:10.1002/jbm.b.34123.

## THE APPLICABILITY OF FURFURYL-GELATIN AS A NOVEL BIOINK FOR TISSUE ENGINEERING APPLICATIONS

**Shweta Anil Kumar<sup>1</sup>, Shane C. Allen<sup>2</sup>, Nishat Tasnim<sup>1</sup>, Tahmina Akter<sup>3</sup>, Shinhye Park<sup>4</sup>, Alok Kumar<sup>1</sup>, Munmun Chattopadhyay<sup>5</sup>, Yoshihiro Ito<sup>4,6</sup>, Laura J. Suggs<sup>2</sup>, and Binata Joddar<sup>1,4,7</sup>**

<sup>1</sup>Inspired Materials & Stem-Cell Based Tissue Engineering Laboratory (IMSTEL), Department of Metallurgical, Materials and Biomedical Engineering, University of Texas at El Paso, 500 W University Avenue, El Paso, TX 79968, USA

<sup>2</sup>Department of Biomedical Engineering, The University of Texas at Austin, 110 Inner Campus Drive, Austin, TX 78712, USA

<sup>3</sup>Department of Chemistry, University of Texas at El Paso, 500 W University Avenue, El Paso, TX 79968, USA

<sup>4</sup>Nano Medical Engineering Laboratory, RIKEN, 2-1 Hirosawa, Wako, Saitama 351-0198, Japan

<sup>5</sup>Department of Biomedical Sciences, Center of Emphasis in Diabetes and Metabolism, Texas Tech University Health Sciences Center, 5001 El Paso Drive, El Paso, TX 79905, USA

<sup>6</sup>Emergent Bioengineering Materials Research Team, RIKEN Center for Emergent Matter Science, 2-1 Hirosawa, Wako, Saitama 351-0198, Japan

<sup>7</sup>Border Biomedical Research Center (BBRC), University of Texas at El Paso, 500 W University Avenue, El Paso, TX 79968, USA

### Abstract

3D bioprinting is an innovative technique in tissue engineering, to create layer-by-layer structures, required for mimicking body tissues. However, synthetic bioinks do not generally possess high printability and biocompatibility at the same time. So, there is an urgent need for naturally derived bioinks that can exhibit such optimized properties. We used furfuryl-gelatin as a novel, visible-light crosslinkable bioink for fabricating cell-laden structures with high viability. Hyaluronic acid was added as a viscosity enhancer and either Rose Bengal or Riboflavin was used as a visible-light crosslinker. Crosslinking was done by exposing the printed structure for 2.5 min to visible light and confirmed using FTIR and rheometry. SEM revealed a highly porous networked structure. Three different cell types were successfully bioprinted within these constructs. Mouse mesenchymal stem cells printed within monolayer and bi-layer sheets showed viability, network formation and proliferation (~5.33 times) within 72 hrs of culture. C2C12 and STO cells were used to print a double layered structure, which showed evidence of the viability of both cells and hetero-cellular clusters within the construct. This furfuryl-gelatin based bioink can be used for tissue engineering of complex tissues and help in understanding how cellular crosstalk happens in vivo during normal or diseased pathology.

## Keywords

furfuryl-gelatin; visible-light crosslinkable bioink; hyaluronic acid; bi-layer sheets; biocompatibility

---

## 1. Introduction

3D bioprinting enables the creation of cell patterns within defined spaces, simultaneously preserving cell function and viability [1]. This technique has the potential to revolutionize the field of regenerative medicine with its endless possibilities [1]. A bioprinter utilizes ‘bioinks’ or materials which mimic an extracellular matrix environment for supporting cell adhesion, proliferation and differentiation [1]. Bioinks distinguish themselves from traditional biomaterials such as polymer networks and foam scaffolds, due to their ability to be deposited as filaments during an additive manufacturing process. However, unlike other additive manufacturing materials such as thermoplastic polymers, ceramics and metals, they require to be processed under milder conditions so as to retain the viability of living cells and to prevent the degradation of bioactive molecules [2]. An ideal bioink is characterized by high shear thinning ability (printability), viscosity, gelation kinetics, biocompatibility, hydration ability and viscoelasticity [3]. They are most often adopted from existing hydrogel biomaterials and are derivatives of natural polymers like gelatin, alginate and fibrin [3]. Hydrogels are preferred over other biomaterials as they are degradable, erodible, absorbable and most importantly biocompatible as well [4]. One of the most commonly used hydrogels is gelatin, which is derived from collagen by hydrolysing the intermolecular, intramolecular and the hydrogen bonds that are known to stabilize the structure of the latter [4–6]. It is primarily comprised of peptides and proteins which are produced by the partial hydrolysis of collagen extracted from the skin, bones and connective tissues of animals like pigs and fish [4–6]. Gelatin is favoured in cell culture on account of its biodegradability, enhanced cell binding ability due to the presence of an RGD-(Arg-Gly-Asp)-sequence [7] and its commercial availability at low cost [8]. It has been shown to have advantages over its parent protein, which includes lower immunogenicity and better solubility in aqueous systems [8]. In addition, gelatin can be crosslinked and modified with the inclusion of other materials, to significantly alter its biochemical properties [9–12] and enhance its mechanical properties [13] *in vitro*. Chemically modified gelatin hydrogels are formed by disulfide crosslinking [14], photo-crosslinking [15, 16] and enzymatic crosslinking [17, 18] to name a few. Numerous studies have applied gelatin methacryloyl (Gel MA)-based hydrogels *in vivo* [19, 20]. However, most chemical modifications that are done to modify gelatin usually render the resultant compound toxic [21, 22].

On the other hand, Son et al. [23] derivatized porcine gelatin by incorporating furfuryl groups. This furfuryl-modified gelatin solution was then mixed with Rose Bengal, a visible-light sensitizer [23]. Irradiation by visible-light crosslinked and gelled the aqueous solution by a photo-oxidation-induced crosslinking mechanism [23]. Furfuryl-gelatin (f-gelatin) had no significant toxicity as it was shown to enhance cell migration and adhesion *in vitro*, in prior studies [23]. In addition, f-gelatin was also shown to be capable of protein immobilization for modification of existing implant surfaces [24] and for *in vivo* tissue

repair applications [15]. In this study, our objective was to determine if an f-gelatin based bioink could be used for bioprinting [25], and for biofabrication of single and double layered cell sheets for tissue engineering [26]. We hypothesized that an f-gelatin based bioink can exhibit properties such as high print fidelity, optimized shear-thinning characteristics and lead to a generation of crosslinked scaffolds with mechanical fidelity and cytocompatibility [27]. To our knowledge, the possibility of using f-gelatin as a bioink has never been explored before. However, it can become a popular bioink [28], due to its superior properties, including the ability to crosslink rapidly when exposed to visible light, cytocompatibility [23] and structural fidelity [15]. To make the f-gelatin based bioink, hyaluronic acid (HA) was added as a viscosity enhancer [29], and Rose Bengal (RB) [30] or Riboflavin (RF) [31] was mixed to act as a photo sensitizer. Both RB and RF can act as visible light crosslinkers. The resultant mixture was homogeneously mixed with cells and printed into structures using a pneumatic extrusion 3D printer, which were photocured for the maintenance of structural integrity. Three different cell types were used in this study. Firstly, sturdy and highly proliferative cells such as mouse mesenchymal stem cells (MSC) [32] were used to bioprint which in turn allowed us to study how the printing process and the selected bioink mixture affected the resultant cell viability, functionality and proliferation. Secondly, C2C12 myoblasts [33] and STO fibroblasts [34] were co-cultured to explore the ability of this technique to serve as a model for studying physiologically relevant cellular interactions, such as those between cardiac myocytes and fibroblasts in vivo [35].

With the possibility of printing multi-layered sheets, this work may eventually open up new vistas in the field of 3D bioprinting of implantable organs by providing an avenue for mimicking complex organs in a dish using a cost-effective and relatively fast method for biofabrication.

## 2. Materials and Methods

### 2.1. Materials

Furfuryl-gelatin (f-gelatin) was made as described below and contributed by our collaborators Drs. Park and Ito from RIKEN, Japan [24, 36]. HA Sodium Salt (mol wt.  $\sim 1.5\text{--}1.8 \times 10^6$  Da) was bought from Sigma-Aldrich (St. Louis, MO, USA). RB, RF and pH strips were procured from ThermoFisher Scientific (Waltham, MA, USA). Dimethyl Sulfoxide (DMSO) was obtained from Sigma.

### 2.2. f-gelatin preparation and characterization

**Preparation and characterization of f-gelatin**—Porcine gelatin powder, furfuryl glycidyl ether (96%) were purchased from Sigma-Aldrich. DMSO was purchased from Duchefa Biochemie (Haarlem, The Netherlands). Sodium hydroxide (NaOH), hydrochloric acid (HCl), acetone and ether were purchased from Duksan Pure Chemical Co., Ltd (South Korea). For preparation, porcine gelatin (2 g) was dissolved in d.d. water (80 mL) and 1 N NaOH solution was added to adjust the pH to 11. Furfuryl glycidyl ether (250  $\mu$ L) was dissolved in DMSO (20 mL) and added to the gelatin solution at room temperature following which the mixture was stirred for 30 h at 65°C. The resulting mixture was adjusted to pH 7 by the addition of 1N HCl solution and dialyzed in DI water for 48 hrs to

purify the f-gelatin using a dialysis membrane with a molecular weight cut-off of 1,000 Da (Spectrum Laboratories Inc., Rancho Dominguez, CA, USA). Following dialysis, the solution was evaporated, and the purified f-gelatin was first washed four times with acetone, once with ether and then dried. Dried f-gelatin was next characterized using <sup>1</sup>H nuclear magnetic resonance (NMR) spectroscopy. Measurement was done using an NMR spectrometer (Gemini 2000, 300 MHz, Varian Inc., Palo Alto, CA, USA). For the analysis, porcine gelatin (control) and f-gelatin were used after dissolving in deuterium oxide (D<sub>2</sub>O, Sigma). The NMR spectra obtained was analysed to confirm derivatization of the gelatin into f-gelatin.

Next the cell compatibility of the synthesized f-gelatin was confirmed (online supplementary information) using MTT assay [37, 38]. Finally the composition of the f-gelatin based mixture was also optimized for visible light induced crosslinking (online supplementary information).

### 2.3. Biofabrication

For biofabrication, a BIOBOT 1 (Biobots, Philadelphia, PA, USA) was used for which we formulated the bioink mixture, as described. A mixture of f-gelatin and HA was made, to which either RB or RF was added, to crosslink the bioprinted structure via visible light-induced crosslinking mechanism [15, 24]. For making 1 ml of this bioink solution, HA (10 mg, 1% w/v) was dissolved in DI water (900 µl, 25°C), followed by the addition and mixing of f-gelatin (100 mg, 10% w/v) at 25°C and then the mixture was heated at 37°C for 1 hr with stirring to facilitate the formation of a homogeneous viscous mixture. The ratio of HA and f-gelatin was maintained at 1:10 and RB (100 µl of 5% (w/v) stock dye solution in DI water added to 900 µl of the remnant mixture to represent a final dye concentration of 0.5% (w/v)) or RF (same as RB) was added as a photo sensitizer, required for the crosslinking after the bioprinting. Cells were added to this mixture as described later, in section 2.5.

This bioink mixture was then loaded into a 10 ml plastic syringe (BD, Franklin lakes, NJ, USA), fitted with a stainless steel blunt-tip dispensing needle (23G, Huaha, Amazon, USA) and extruded using low extrusion pressure (Table 1). Patterns printed using this bioink were designed using SolidWorks (Concord, MA, USA) and saved as .stl files. Briefly, two patterns, namely rectangular and circular structures, were printed in 100 mm × 15 mm petri dishes (ThermoFisher). The .stl files were transferred to the Repetier Host program available via BIOBOT 1 server and converted into a g-code (Table 1). These g-code files were uploaded and used for printing using parameters in Table 1. The printed structures were immediately exposed to visible light for 2.5 min for crosslinking (400 nm wavelength at 100% intensity, Intelli-Ray 600, Uvitron International, West Springfield, MA, USA).

The rectangular sheet structure, initially printed as a monolayer, was further expanded by printing a secondary layer to demonstrate the feasibility of fabricating a bi-layer structure using the f-gelatin based bioink (Table 1). For printing bi-layer sheet structures, the bottom layer was first printed using bioink (with cells) with RB and crosslinked for 2.5 min. A second layer was printed atop the former, using bioink (with cells) with RF, and crosslinked similarly for an additional 2.5 min. The necessity for addition of two different dyes, RB and RF was to highlight a distinct bilayer structure that could be printed easily.

## 2.4. Characterization of the bioink and the post-crosslinked structure

**Rheology of bioink**—Gels for rheometry were formed as described earlier and cut using a biopsy punch (~1 mm deep, 8 mm diameter). The gels were pre-swollen in 1X PBS before testing. Oscillatory shear stress rheometry was performed (1% strain, 0.5 – 50 Hz) using an Anton-Paar MCR101 rheometer (Anton-Paar, Graz, Austria) with an 8-mm parallel plate geometry. The strain and frequency range were analysed within the linear viscoelastic range of the gels by frequency sweeps. Elastic modulus was calculated through complex shear modulus with storage and loss modulus, and complex viscosity was measured at 1.99 Hz for all samples, as done earlier [39].

**Fourier transform infrared spectroscopy analysis**—Fourier transform infrared spectroscopy (FTIR) was used to reveal information about the crosslinked structure after exposure to visible light irradiation, in comparison with the non-crosslinked f-gelatin and the HA. Attenuated total reflectance (ATR)-FTIR spectra of representative samples were acquired using a Perkin-Elmer, Spectrum 100, Universal ATR Sampling Accessory within the range of 650–3650  $\text{cm}^{-1}$  in transmittance mode, as done before [40]. Spectral manipulations were performed using the spectral analysis software GRAMS/32 (Galactic Industries Corp., Salem, NH, USA). External reflection FTIR was recorded on a Specac grazing angle accessory using an s-polarized beam at an angle of incidence of 40° and a mercury cadmium telluride (MCT/A) detector. A piranha-treated silicon wafer was used as the background.

**Swelling Analysis**—To account for the hydration parameters of the crosslinked hydrogel structure leading to swelling, gels were allowed to swell to equilibrium for 5 days in Dulbecco Modified Eagle's Medium (DMEM, pH = 7, 25°C) following published protocols [41]. Three similar printed sheet structures were crosslinked and stored at -80°C (12 hrs) following which the samples were freeze-dried using a VirTis BenchTop Pro Freeze Dryer with Omnitronics (SP Scientific, Warminster, PA, USA). These freeze-dried samples were weighed ( $W_0$ ) and then immersed in DMEM and the increase in weight was recorded periodically ( $W_t$ ) after every 24 hrs till 5 days. The swelling ratio was calculated using the following equation (1), where  $D_s$  was the degree of swelling,  $W_0$  and  $W_t$  were the weights of the samples in the dry and swollen states respectively [41].

$$D_s = (W_t - W_0)/W_0 \quad (1)$$

**Scanning Electron Microscopy**—En-face and cross-sectional images of the dried gels were acquired using scanning electron microscopy (SEM), following published procedures [41]. For en-face imaging, uniformly sized gels were made and air-dried in a chemical fume hood overnight and visualized using SEM (Hitachi TM-1000 Tabletop Microscope, Tokyo, Japan) at 504× magnification. For imaging of the cross-sections, uniformly sized gels were made, freeze-dried and sputter-coated with gold/palladium (2–3 min) in a sputter coater (Gatan Model 682 Precision etching coating system, Pleasantown, CA, USA) and visualized using SEM (S-4800, Hitachi, Japan) at voltages of 5 kV at 80× and 100× magnification. En-

face and cross-sectional SEM images were analysed using ImageJ software to determine the average pore size and the apparent porosity (%), respectively. Apparent porosity was calculated by the following formula (2) below.

$$App. \text{ porosity} = \frac{\text{total area covered by pores (sq. } \mu\text{m)}}{\text{total sample area of the cross section (sq. } \mu\text{m)}} * 100 \quad (2)$$

## 2.5. Biocompatibility

Strain C57BL/6 Mouse MSC (catalog #: MUBMX-01001) and Growth Medium (complete growth medium, catalog #: MUXMX-90011) were obtained from Cyagen, Santa Clara, CA, USA. The cells were cultured, passaged and stabilized for at least 6 passages before being used in bioprinting. For bioprinting with cells, bioink was prepared as described earlier (section 2.3) to which cells were added. Prior to addition in the bioink mixture, the mouse MSCs were labelled with PKH67 green fluorescent dye (Sigma), or PKH26 red fluorescent dye (Sigma) following manufacturer's protocols. Both dyes are used for cell tracking purposes in vitro or in vivo [42]. These labelled mouse MSCs were mixed with bioink ( $1 \times 10^7$  cells/ml) and loaded into a 10 ml syringe for extrusion and printing. The printed, crosslinked, cell-laden gel structures were then incubated with 5 ml of complete growth medium for mouse MSC and incubated ( $37^\circ\text{C}$ , 5%  $\text{CO}_2$ ) for a period of up to 72 hrs. The cell-laden bioprinted structures, both mono- and bi-layered sheets were analysed using inverted confocal fluorescence microscopy (ZEISS LSM 700 confocal, Germany) after 5 days of culture, to confirm cell retention and density. To confirm that the printing process did not adversely affect cellular viability, Hoechst 33342 (Thermo Scientific Pierce), a 20 mM aqueous stock solution of a fluorescent stain was used to detect and image cells, immediately after printing (within 24 hrs).

In addition, to check the capability of this method for co-layering, two different cell types namely, STO fibroblasts (STO, ATCC® CRL-1503™) and C2C12 myoblasts (C2C12, ATCC® CRL-1772™), both from American Type Culture Collection (ATCC), Manassas, VA, USA, were used. Both cells were cultured and stabilized for at least 6 passages using DMEM/F12 medium supplemented with 5% foetal bovine serum (FBS, Invitrogen, Carlsbad, CA, USA) before being used in bioprinting. For bioprinting of a bi-layer structure with STO (bottom) and C2C12 (top), two separate bioinks were prepared by adding  $1 \times 10^7$  cells/ml of STO or C2C12 respectively, to the f-gelatin mixture and loaded into two separate 10 ml syringes for extrusion and printing. First, the STO encapsulated layer was printed, and crosslinked, above which the C2C12 layer was deposited and crosslinked to generate a composite bi-cellular construct. These structures were then incubated with 5 ml of DMEM/F12 and incubated ( $37^\circ\text{C}$ , 5%  $\text{CO}_2$ ) for a period of up to 48 hrs. Then they were fixed with paraformaldehyde (Sigma) for 30 min ( $25^\circ\text{C}$ ) and then permeabilized with 0.2% Triton X-100/phosphate buffered saline (PBS) for 15 min. After blocking with 1% bovine serum albumin (BSA/PBS, Sigma) for 30 min at room temperature, the samples were incubated with a mouse monoclonal antibody against Anti-MyoD1 antibody [5.2F] followed by a goat polyclonal secondary antibody to mouse IgG1 - heavy chain (FITC) (Abcam, Cambridge, UK). The STO cells were not labelled with any dye. The cells were then imaged

using a confocal fluorescence microscopy (Olympus IX81 inverted fluorescence motorised microscope, Japan) to confirm the retention of both cell types and their possible co-localization in a single plane of view, within the printed structure.

**Flow Cytometry analysis**—To estimate cell proliferation and overall biocompatibility of the printed construct, the cells were pre-stained using Cell Trace Violet, proliferation kit (Invitrogen, Carlsbad, CA, USA) using manufacturer's protocols. These pre-stained cells were mixed with the bioink ( $1 \times 10^7$  cells/ml) and printed into monolayer sheets and cultured for 24 hrs, and 72 hrs respectively ( $37^\circ\text{C}$ , 5%  $\text{CO}_2$ ). After 24- and 72-hrs, cell-gel samples were treated using Trypsin-EDTA (0.25%, phenol red) (ThermoFisher), cells were detached, extracted and processed for flow cytometry, by fluorescence assorted cell sorting (FACS). Extracted cells were fixed and processed further for FACS (Beckman Coulter Gallios Flow Cytometer, Brea, CA, USA) using excitation and emission wavelengths of 405 and 450 nm respectively. Positive controls included pre-stained cells grown on plastic petri dishes for 72 hrs. Negative controls included non-stained cells grown on plastic petri dishes for 72 hrs.

## 2.6. Sample size and data

All samples were present in triplicate unless otherwise mentioned. Numerical data are expressed as the mean  $\pm$  standard deviation.

## 3. Results

The  $^1\text{H}$  NMR spectrum of f-gelatin is shown in Supplementary Figure 1A, B (online supplementary information). Shown in Supplementary Figure 2, is the estimated viability (% absorbance) of 3T3-L1 fibroblast cells treated with f-gelatin measured using the MTT assay. No significant difference was noted among the values estimated from cells treated with f-gelatin solution versus controls (not treated with f-gelatin). This confirmed that the f-gelatin solution was not cytotoxic, in line with previously published results [23]. Shown in Supplementary Figure 3, is 10% (w/v) and 1% (w/v) f-gelatin mixed with RB (Pink) or RF (Yellow). Controls that were not photocured dispersed readily in water, whereas 10% (w/v) f-gelatin mixed with either RB or RF retained their size and shape for 8 days (right), while 1% (w/v) f-gelatin structures dissolved in the interim. After 14 days, the photocured f-gelatin samples could be recovered from the bottom of the petri dishes. This confirmed visible light-induced crosslinking and stability of 10% (w/v) photo-cured f-gelatin. This result lead to optimization of the bioink mixture based on 10% f-gelatin (w/v) for printing. However this f-gelatin and RB/RF mixture did not provide sufficient viscosity and shear thinning properties for printing (Supplementary Figure 4). Therefore a secondary material had to be added as a viscosity enhancer [43]. HA, a well-known glycosaminoglycan [44], was added at a concentration of 1% (w/v) and mixed with the remaining bioink mixture [45]. Our goal was to add HA to enhance viscosity, but keep its content minimal such that it would not interfere with the crosslinking mechanism of the f-gelatin in the presence of RB or RF.

As shown in Figure 1A, the bioink mixture (without cells) with added HA, was relatively viscous and had to be scooped out with the aid of a fine tipped spatula, to load in a syringe

prior to printing. However, the hydrogel exhibited good shear thinning characteristics as only a relatively low-pressure range was required to extrude the bioink into the desired structures (Figure 1B, C, D). The printed structures could be rapidly crosslinked by exposure to visible light and exhibited structural fidelity compared to the non-crosslinked structures (Figure 1B, C, D). The structures printed from multiple experiments exhibited consistency. The bi-layered sheet structures showed two distinct layers, one atop the other, distinguishable by their distinct colours (Figure 1D), yet appearing as a composite structure when examined at its cross-section (Figure 1D).

From the rheometric analysis of the hydrogels, it was determined that the strain and frequency range were within the linear viscoelastic range of the gels by amplitude and frequency sweeps (Figure 2). We were able to generate crosslinked gels of elastic modulus  $1.7 \pm 0.3$  kPa and complex viscosity compared to the non-crosslinked pre-hydrogels which revealed an elastic modulus of  $1.4 \pm 0.05$  kPa. Additionally, crosslinking increased the complex viscosity of the gels from  $206.25 \pm 11.79$  to  $319.7 \pm 43.01$  Pa-s.

FTIR spectrum of a representative sample was analysed to confirm the formation of the crosslinked structure of f-gelatin, HA and RB under visible light irradiation (Figure 3A). As shown in the reaction mechanism (Supplementary Figure 1B), a double bond was formed in the crosslinked product in the furan ring of f-gelatin which corresponds to the band of C=C at  $1447\text{ cm}^{-1}$ . The spectrum also depicted other functional group peaks at different bands. The peak at  $2942\text{ cm}^{-1}$  represents the C-N stretching peak, the C-O-C peak of the aryl ether was at  $1234\text{ cm}^{-1}$  shifted from  $1215\text{ cm}^{-1}$  in the non-crosslinked f-gelatin (Figure 3B) for the new bond formation [46]. The aryl ether peak is represented by bands at  $1039\text{ cm}^{-1}$  and at  $1075\text{ cm}^{-1}$ . The presence of the broad peak ( $\sim 3000\text{--}3400\text{ cm}^{-1}$ ) is the representation of the vibrational -OH stretching peak of the -COOH group in the Hyaluronic Acid (HA), also found in the pure HA (Figure 3C). The absence of oxy-HA peak around  $1697\text{ cm}^{-1}$  in the crosslinked sample confirmed that HA was not oxidized during the rapid irradiation of the crosslinking process [47]. The C-N stretching peak was present at  $1363\text{ cm}^{-1}$  in both pure HA and f-gelatin structure.

The swelling kinetics and behaviour of bioprinted crosslinked hydrogels is depicted in Figure 4. For all samples tested, the maximum swelling was observed at 24 hrs of incubation after which the swelling ratios remained relatively unchanged throughout the remaining incubation period of 5 days. Although data reported was from 5 days of observation and analysis, the stored gels did not degrade until 21 days in culture following this observation. Thus, the bioprinted crosslinked constructs are expected to maintain their structural fidelity when implanted in vivo for a sustainably long period of time.

SEM en-face images revealed a highly organized and striated structure with repeating chain like units (Figure 5A). However, the cross-sectional images revealed a highly porous structure with interconnected pores and an average pore size of  $142.20 \pm 1.08\text{ }\mu\text{m}$  (Figure 5B). The average apparent porosity was estimated to be  $21 \pm 0.45\%$ . Results led us to conclude that there was significant porosity for nutrient and water intake into these constructs during culture.



Densely packed Hoechst-dye stained cells (Figure 6A) confirmed cellular viability post printing thereby affirming that neither the printing process, the bioink mixture nor the crosslinking had adversely affected cell viability, post printing. This cell density appeared to have reduced when samples were imaged after 5 days (Figure 6B). This may have been due to the swelling of the gels which allowed cells to migrate out of the structure into other areas of the tissue culture petri dish.

Pre-stained mouse MSC when printed within monolayer sheets, showed the evidence of cell retention after 5 days of culture (Figure 6B, Supplementary Figure 5) when stained with either PKH67 or PKH26. Similar results were observed when the labelled mouse MSC (PKH26: red) were printed within bi-layer sheets and cultured for the same duration (Supplementary Figure 5). There were no apparent differences in the cell density in both cases (Supplementary Figure 5) even though cells in the bi-layer (bottom) were subjected to photo crosslinking by visible light for a longer duration (5 min) compared to the monolayer (2.5 min). PKH67 labelled cells could not be used for visualization within the bi-layers, as the dye was also absorbed by the gels exhibiting high background fluorescence (images not included). The average area occupied by the cells was estimated to be  $33.8 \pm 9.91\%$  of the total area. The presence of a large number of cells retained, even after 5 days of incubation, validated that cells could survive the process of extrusion based 3D printing, crosslinking and culture thereafter.

Results from FACS analysis (Figure 7, Supplementary Figure 6) showed that after 24 hrs of culture, 9.1% of the total number of cells encapsulated in the bioprinted construct had proliferated in comparison to controls (unstained, 0.3%). After 72 hrs of culture, 48.6% of the cells were found to have proliferated (in comparison with 32% proliferating cell population in positive controls, Supplementary Figure 6, 7) confirming the biocompatibility of the bioink and viability of cells in these printed constructs. Further, the occurrence of multiple peaks (Figure 7) revealed the presence of consecutive proliferating generations of cells, in the bioprinted constructs. In future, we will analyse how this hydrogel modulates cellular functions such as stem cell differentiation (MSC) into targeted tissues such as cartilage or bone.

Figure 8 shows the evidence of STO and C2C12 (Figure 8C, E) encapsulated within the same structure (and Supplementary Figure 8). Interestingly, we noted STO cells in the same plane as C2C12, even though they were confined to their respective layers (bottom and top) during the fabrication process (Figure 8A, B and Supplementary Figure 8 A, B). This probably was due to their interaction at the junction of the two layers containing two different cell types respectively. The morphology of both C2C12 [48] and STO [49] cells were similar to images reported in others published works. This data provided strong evidence of the feasibility of culturing two different cell types within the same bioprinted construct, which unified as a single structure (Figure 8D) and did not fall apart into two separate layers during culture and incubation.

## 4. Discussion

The past few years have witnessed a profound advancement in the use of 3D printing in the field of regenerative medicine [3]. This growth has been accelerated by the emergence of new bioinks for printing, leading to the possibility of creating high resolution tissues and organs [3]. The present study demonstrates the applicability of using an f-gelatin and HA based bioink for the biofabrication of cellular sheets geared towards tissue engineering applications. The f-gelatin consisted mainly of porcine gelatin, modified by the incorporation of a furfural group [23, 24]. Earlier studies on this f-gelatin led to the development of a scaffold for the treatment of in vivo osteochondral injuries and defects [15]. F-gelatin was rapidly crosslinked by visible light with RB, a light sensitizer, and was kept gelled for 3 weeks submerged in saline at 37°C [15]. This prompted us to further explore the properties of f-gelatin as a novel bioink as it can be rapidly crosslinked in the presence of visible light to maintain structural fidelity [27]. However, it needs to be mixed with some viscosity enhancer [50] such as HA. When used in tandem with f-gelatin, HA imparted the necessary viscosity and shear thinning to the bioink, followed by structural integrity and stiffness to the printed crosslinked structure, although HA was not chemically crosslinked with the remaining bioink mixture. Nonetheless, with such a high content of HA in the bioink (1% w/v) it is reasonable to suggest that it might have also played a vital role in maintaining cellular biocompatibility and other biological effects on the cells cultured [43, 44]. Besides, a high content of gelatin, as in this study is also believed to exert cytoprotective effects on cells cultured [15].

Our long-term goal is to biofabricate multi-layered, multi-cellular tissue structures which can be used for mimicking in vivo tissues including healthy tissues such as the myocardium or diseased cancer tissues. As a first step, we fabricated bi-layered sheets, laden with cells which were rapidly crosslinked, cultured with growth medium for a sustainable period in vitro. The crosslinked hydrogels had a viscosity comparable to tumours in vivo [51]. Generally, polyacrylamide hydrogels with elastic moduli ranging from 1 to 25 kPa have been used as scaffolds, to study cardiomyocyte behaviour in vitro. Although the elastic moduli for our crosslinked gels fit well within this range, they need to be closer to 9 kPa in order to more closely mimic the properties of a native myocardium [52]. Therefore, in the future, we will work on including additives such as carbon nanotubes to improve the stiffness of the printed cell gel constructs [41], which can also make the scaffolds electrically active and conductive [53, 54]. Besides, the HA could be chemically crosslinked with the entire hydrogel mixture, adding to its overall stiffness. Structurally, the bi-layered composite gel behaved as one solid hydrophilic structure, and no gaps at the junction could be detected. Further, the cells which were confined to their respective layers (top and bottom) during printing, showed migration within the bi-layer gel after sustained culture. This implies that this bioprinting strategy can be applied to mimic complex tissues containing various cells in different anatomical locations, such as in the cardiac wall [55].

As the crosslinked gels were extremely stable when exposed to long term culture, they can be extremely effective for in vivo studies as well [15]. The swelling data for these crosslinked gels are also consistent with other's published values of photo-crosslinked [56] and gelatin-based hydrogels [57]. In comparison with other types of hybrid gelatin hydrogels

(e.g. gelatin methacrylamide (Gel-MA) and arginine-based unsaturated non-peptide polycations (Arg-UPEA) [57]), these gels produced via a simple crosslinking mechanism can preserve their structural integrity for a long period, which will be beneficial for in vivo use. Besides, growth factors or other chemokines can be mixed and crosslinked along with the hydrogel for releasing into the culture or in vivo, as desired [15].

Although the total area populated by the cells appeared to be low, initially, this probably led to the proliferation and migration of cells during culture which may have added to enhance the stability and integrity of the cell-gel construct. The mouse MSC proliferated more in the gel compared to plastic wells, which implied that a 3D scaffold is effective compared to a flat surface [58]. Further f-gelatin based hydrogels are known to be extremely favourable towards promoting cell growth [23].

We aim to deliver complex 3D tissues-on-a-dish, in the future. Towards this end, we desire to fabricate cardiac wall tissue in vitro utilizing 3D bioprinting, which can then be implanted directly in vivo or exploited in vitro for the screening of pharmaceutical cardiotoxicity. So in this study, as a proof of principle we co-cultured two different cell types, namely STO fibroblasts, and C2C12 myoblasts, often used to model the response of myocytes for cardiac tissue engineering applications. Evidence of co-localization of both of these cell types in a single plane implied that this technique could be applied to study physiologically relevant interactions between cardiac fibroblasts (CF) and cardiomyocytes (CM) that has been well established in vitro [35], and is implied in vivo [35]. In the context of heart disease, enhanced CM:CF coupling may influence the electrical activity of the myocytes leading to cardiac arrhythmias [59, 60]. However, better cell co-culture systems are needed to enable studies probing into mechanisms resulting from the interactions between these two significant cell types, CF and CM found in the myocardium. This is because native 'bulk' tissue studies are associated with significant challenges including lack of visual inspection and monitoring [5]. This gives rise to an immediate need for intermediate level thin sections of biological model systems for probing into hetero-cellular coupling between CF and CM and its resultant effects. Our method of co-culturing cells using 3D bioprinting may prove to be novel and extremely useful for this purpose. Results can provide unexpected advances in our understanding of the interplay between multiple cell types that make up the heart wall.

In this study, we did not explore strategies for promoting vascularization, however in future studies that will be a major focus, for incorporation within complex multi-layered 3D printed constructs consisting of multiple cell types, such as endothelial progenitor cells [61]. Further we will also attempt fabrication of architecturally complex structures such as lattice or tissue structures with this bioink mixture.

In conclusion, we showed the applicability of f-gelatin as a novel, biocompatible bioink for biofabrication of cell-gel constructs with enhanced fidelity. Although both synthetic and natural materials have been proposed to generate suitable tissue engineering grafts, the ideal material or scaffold for repair and regeneration of cardiac tissue is not yet known [62]. We hope to utilize this f-gelatin-based bioink for mimicking myocardial tissue, by printing layer-by-layer with the actual cardiac cells, namely cardiomyocytes, fibroblasts and

endothelial cells [55]. This will help generate a functional cardiac patch that can be used for drug cytotoxicity screening [63], or exploring triggers for heart diseases in vitro [64].

## Supplementary Material

Refer to Web version on PubMed Central for supplementary material.

## Acknowledgments

The authors acknowledge technical assistance received from the following individuals: Ivan Hernandez (IMSTEL), Dr. Monica Michel and Dr. Katja Michael at UTEP. We gratefully acknowledge the support from Dr. Armando Varella (UTEP BBRC) and Elsa Morales (Texas Tech University Health Sciences Center) for assistance in FACS analysis and confocal imaging. We thank the high school student, Estevan Mesa (CHS, EPISD) for making the bioink mixture. We acknowledge the support received from Ricky Solórzano (BioBots) for efficiently running the BIOBOT 1 for all our experiments. B.J acknowledges NIH BUILD Pilot 8UL1GM118970-02 and NIH 1SC2HL134642-01 for funding support and the NSF-PREM program (DMR 1205302) for materials and supplies. N.T acknowledges the Anita Mochen Loya fellowship at UTEP. The authors also acknowledge the use of the Core Facility at Border Biomedical Research Consortium at UTEP supported by NIH-NIMHD-RCMI Grant No. 2G12MD007592.

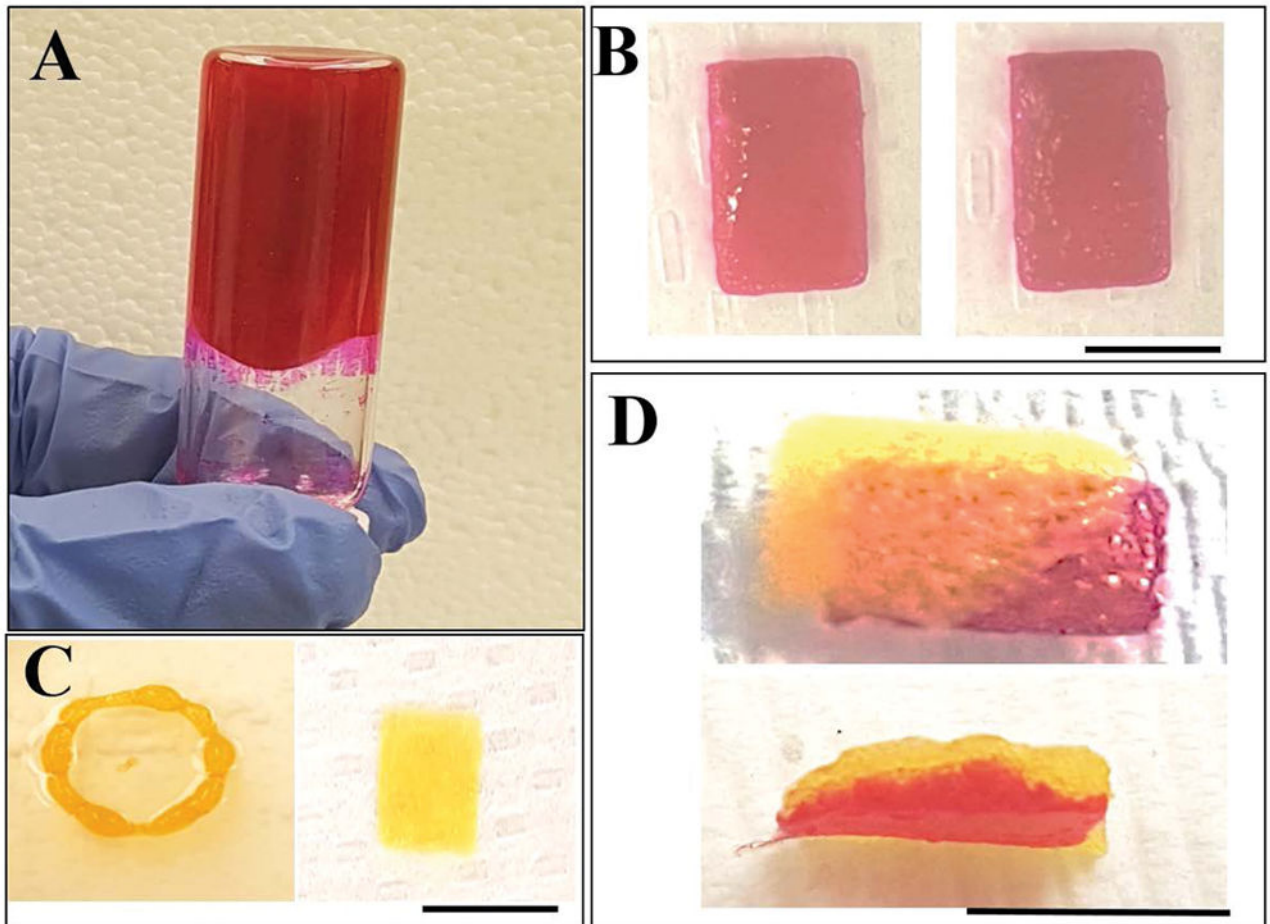
## References

- Murphy SV, Atala A. *3D bioprinting of tissues and organs*. Nature biotechnology. 2014; 32(8):773–785.
- Yan Y, et al. Fabrication of viable tissue-engineered constructs with 3D cell-assembly technique. Biomaterials. 2005; 26(29):5864–5871. [PubMed: 15949552]
- Ferris CJ, et al. Bio-ink for on-demand printing of living cells. Biomaterials Science. 2013; 1(2): 224–230.
- Drury JL, Mooney DJ. Hydrogels for tissue engineering: scaffold design variables and applications. Biomaterials. 2003; 24(24):4337–4351. [PubMed: 12922147]
- Kang H-W, Tabata Y, Ikada Y. Fabrication of porous gelatin scaffolds for tissue engineering. Biomaterials. 1999; 20(14):1339–1344. [PubMed: 10403052]
- Lee KY, Mooney DJ. Hydrogels for tissue engineering. Chemical reviews. 2001; 101(7):1869–1880. [PubMed: 11710233]
- Boskey A, et al. Osteopontin-hydroxyapatite interactions in vitro: inhibition of hydroxyapatite formation and growth in a gelatin-gel. Bone and mineral. 1993; 22(2):147–159. [PubMed: 8251766]
- Gorgieva, S, Kokol, V. INTECH open access publisher Croatia. 2011. Collagen-vs. gelatine-based biomaterials and their biocompatibility: review and perspectives.
- Angele P, et al. Engineering of osteochondral tissue with bone marrow mesenchymal progenitor cells in a derivatized hyaluronan-gelatin composite sponge. Tissue engineering. 1999; 5(6):545–553. [PubMed: 10611546]
- Ifkovits JL, Burdick JA. Review: photopolymerizable and degradable biomaterials for tissue engineering applications. Tissue engineering. 2007; 13(10):2369–2385. [PubMed: 17658993]
- Ovsianikov A, et al. Laser fabrication of three-dimensional CAD scaffolds from photosensitive gelatin for applications in tissue engineering. Biomacromolecules. 2011; 12(4):851–858. [PubMed: 21366287]
- Sakai S, et al. An injectable, in situ enzymatically gellable, gelatin derivative for drug delivery and tissue engineering. Biomaterials. 2009; 30(20):3371–3377. [PubMed: 19345991]
- Van Den Bulcke AI, et al. Structural and rheological properties of methacrylamide modified gelatin hydrogels. Biomacromolecules. 2000; 1(1):31–38. [PubMed: 11709840]
- Shu XZ, et al. Disulfide-crosslinked hyaluronan-gelatin hydrogel films: a covalent mimic of the extracellular matrix for in vitro cell growth. Biomaterials. 2003; 24(21):3825–3834. [PubMed: 12818555]

15. Mazaki T, et al. A novel, visible light-induced, rapidly cross-linkable gelatin scaffold for osteochondral tissue engineering. *Scientific reports*. 2014; 4:4457. [PubMed: 24662725]
16. Zhao X, et al. Photocrosslinkable gelatin hydrogel for epidermal tissue engineering. *Advanced healthcare materials*. 2016; 5(1):108–118. [PubMed: 25880725]
17. Lemes GF, et al. Enzymatically crosslinked gelatin coating added of bioactive nanoparticles and antifungal agent: Effect on the quality of Benitaka grapes. *LWT-Food Science and Technology*. 2017
18. Yang G, et al. Enzymatically crosslinked gelatin hydrogel promotes the proliferation of adipose tissue-derived stromal cells. *PeerJ*. 2016; 4:e2497. [PubMed: 27703850]
19. Daly AC, et al. A comparison of different bioinks for 3D bioprinting of fibrocartilage and hyaline cartilage. *Biofabrication*. 2016; 8(4):045002. [PubMed: 27716628]
20. Levato R, et al. The bio in the ink: cartilage regeneration with bioprintable hydrogels and articular cartilage-derived progenitor cells. *Acta Biomater*. 2017; 61:41–53. [PubMed: 28782725]
21. Kuo W-T, et al. Surface modification of gelatin nanoparticles with polyethylenimine as gene vector. *Journal of Nanomaterials*. 2011; 2011:28.
22. Lai J-Y. Biocompatibility of chemically cross-linked gelatin hydrogels for ophthalmic use. *Journal of Materials Science: Materials in Medicine*. 2010; 21(6):1899–1911. [PubMed: 20238149]
23. Son TI, et al. Visible light-induced crosslinkable gelatin. *Acta Biomaterialia*. 2010; 6(10):4005–4010. [PubMed: 20580950]
24. Park SH, et al. Preparation of photocured azidophenyl-fish gelatin and its capturing of human epidermal growth factor on titanium plate. *Journal of Applied Polymer Science*. 2013; 127(1):154–160.
25. Pati F, et al. Printing three-dimensional tissue analogues with decellularized extracellular matrix bioink. *Nature communications*. 2014:5.
26. Jakab K, et al. Tissue engineering by self-assembly and bio-printing of living cells. *Biofabrication*. 2010; 2(2):022001. [PubMed: 20811127]
27. Chimene D, et al. Advanced bioinks for 3D printing: A materials science perspective. *Annals of biomedical engineering*. 2016; 44(6):2090–2102. [PubMed: 27184494]
28. Müller M, et al. Nanostructured pluronic hydrogels as bioinks for 3D bioprinting. *Biofabrication*. 2015; 7(3):035006. [PubMed: 26260872]
29. Monheit GD, Coleman KM. Hyaluronic acid fillers. *Dermatologic therapy*. 2006; 19(3):141–150. [PubMed: 16784513]
30. Shrestha A, Hamblin MR, Kishen A. Photoactivated rose bengal functionalized chitosan nanoparticles produce antibacterial/biofilm activity and stabilize dentin-collagen. *Nanomedicine: Nanotechnology, Biology and Medicine*. 2014; 10(3):491–501.
31. Wollensak G, et al. Hydration behavior of porcine cornea crosslinked with riboflavin and ultraviolet A. *Journal of Cataract & Refractive Surgery*. 2007; 33(3):516–521. [PubMed: 17321404]
32. Lin X, et al. MiR-335-5p Promotes Chondrogenesis in Mouse Mesenchymal Stem Cells and Is Regulated Through Two Positive Feedback Loops. *Journal of Bone and Mineral Research*. 2014; 29(7):1575–1585. [PubMed: 24347469]
33. Radisic M, et al. High-density seeding of myocyte cells for cardiac tissue engineering. *Biotechnology and bioengineering*. 2003; 82(4):403–414. [PubMed: 12632397]
34. Hoveizi E, et al. Functionalisation and surface modification of electrospun polylactic acid scaffold for tissue engineering. *Cell biology international*. 2014; 38(1):41–49. [PubMed: 24030862]
35. Kohl P, Gourdie RG. Fibroblast–myocyte electrotonic coupling: does it occur in native cardiac tissue? *Journal of molecular and cellular cardiology*. 2014; 70:37–46. [PubMed: 24412581]
36. Park, S-h; , et al. Preparation of a visible light-reactive low molecular-O-carboxymethyl chitosan (LM-O-CMCS) derivative and applicability as an anti-adhesion agent. *Macromolecular research*. 2011; 19(9):921.
37. Marks DC, et al. The MTT cell viability assay for cytotoxicity testing in multidrug-resistant human leukemic cells. *Leukemia research*. 1992; 16(12):1165–1173. [PubMed: 1361210]

38. Spielmann H, et al. The embryonic stem cell test, an in vitro embryotoxicity test using two permanent mouse cell lines: 3T3 fibroblasts and embryonic stem cells. *In Vitro Toxicology*. 1997; 10:119–128.
39. Stowers RS, Allen SC, Suggs LJ. Dynamic phototuning of 3D hydrogel stiffness. *Proceedings of the National Academy of Sciences*. 2015; 112(7):1953–1958.
40. Tasnim N, Kumar A, Joddar B. Attenuation of the in vitro neurotoxicity of 316L SS by graphene oxide surface coating. *Materials Science and Engineering: C*. 2017; 73:788–797. [PubMed: 28183673]
41. Joddar B, et al. Development of functionalized multi-walled carbon-nanotube-based alginate hydrogels for enabling biomimetic technologies. *Scientific reports*. 2016;6. [PubMed: 28442741]
42. Nagyova M, et al. A comparative study of PKH67, DiI, and BrdU labeling techniques for tracing rat mesenchymal stem cells. *In Vitro Cellular & Developmental Biology-Animal*. 2014; 50(7): 656–663. [PubMed: 24737277]
43. Toole BP. Hyaluronan: from extracellular glue to pericellular cue. *Nature Reviews Cancer*. 2004; 4(7):528. [PubMed: 15229478]
44. Toole, BP. *Seminars in cell & developmental biology*. Elsevier; 2001. Hyaluronan in morphogenesis.
45. Joddar B, Ramamurthi A. Fragment size-and dose-specific effects of hyaluronan on matrix synthesis by vascular smooth muscle cells. *Biomaterials*. 2006; 27(15):2994–3004. [PubMed: 16457881]
46. Montiel-Herrera M, et al. N-(furfural) chitosan hydrogels based on Diels–Alder cycloadditions and application as microspheres for controlled drug release. *Carbohydrate polymers*. 2015; 128:220–227. [PubMed: 26005158]
47. Sheu SY, et al. Biological characterization of oxidized hyaluronic acid/resveratrol hydrogel for cartilage tissue engineering. *Journal of Biomedical Materials Research Part A*. 2013; 101(12): 3457–3466. [PubMed: 23595953]
48. Contreras-Shannon V, et al. Clozapine-Induced Mitochondria Alterations and Inflammation in Brain and Insulin-Responsive Cells. *PLOS ONE*. 2013; 8(3):e59012. [PubMed: 23527073]
49. Park Y-G, et al. Effects of Feeder Cell Types on Culture of Mouse Embryonic Stem Cell In Vitro. *Development & Reproduction*. 2015; 19(3):119–126. [PubMed: 27004268]
50. Schuurman W, et al. Gelatin-methacrylamide hydrogels as potential biomaterials for fabrication of tissue-engineered cartilage constructs. *Macromolecular bioscience*. 2013; 13(5):551–561. [PubMed: 23420700]
51. Levental KR, et al. Matrix crosslinking forces tumor progression by enhancing integrin signaling. *Cell*. 2009; 139(5):891–906. [PubMed: 19931152]
52. Boothe SD, et al. The Effect of Substrate Stiffness on Cardiomyocyte Action Potentials. *Cell biochemistry and biophysics*. 2016; 74(4):527–535. [PubMed: 27722948]
53. Martinelli V, et al. Carbon nanotubes promote growth and spontaneous electrical activity in cultured cardiac myocytes. *Nano letters*. 2012; 12(4):1831–1838. [PubMed: 22432413]
54. Saha A, Jiang C, Martí AA. Carbon nanotube networks on different platforms. *Carbon*. 2014; 79:1–18.
55. Wessels A, Sedmera D. Developmental anatomy of the heart: a tale of mice and man. *Physiological genomics*. 2003; 15(3):165–176. [PubMed: 14612588]
56. Jeon O, et al. Photocrosslinked alginate hydrogels with tunable biodegradation rates and mechanical properties. *Biomaterials*. 2009; 30(14):2724–2734. [PubMed: 19201462]
57. Sun X, et al. Development of a hybrid gelatin hydrogel platform for tissue engineering and protein delivery applications. *Journal of Materials Chemistry B*. 2015; 3(30):6368–6376.
58. Griffith LG, Swartz MA. Capturing complex 3D tissue physiology in vitro. *Nature reviews. Molecular cell biology*. 2006; 7(3):211. [PubMed: 16496023]
59. McArthur, L., et al. *Electrical consequences of cardiac myocyte: fibroblast coupling*. Portland Press Limited; 2015. 513–518.

60. Thompson SA, et al. Mechanical coupling between myofibroblasts and cardiomyocytes slows electric conduction in fibrotic cell monolayers. *Circulation*. 2011; 123(19):2083–2093. [PubMed: 21537003]
61. Asahara T, et al. Isolation of putative progenitor endothelial cells for angiogenesis. *Science*. 1997; 275(5302):964–966. [PubMed: 9020076]
62. Malafaya PB, Silva GA, Reis RL. Natural–origin polymers as carriers and scaffolds for biomolecules and cell delivery in tissue engineering applications. *Advanced drug delivery reviews*. 2007; 59(4):207–233. [PubMed: 17482309]
63. Hansen A, et al. Development of a drug screening platform based on engineered heart tissue. *Circulation research*. 2010; 107(1):35–44. [PubMed: 20448218]
64. Hirt MN, Hansen A, Eschenhagen T. Cardiac Tissue Engineering. *Circulation research*. 2014; 114(2):354–367. [PubMed: 24436431]



**Figure 1.**

(A) Bioink (no cells) showing a viscous mixture prior to crosslinking.

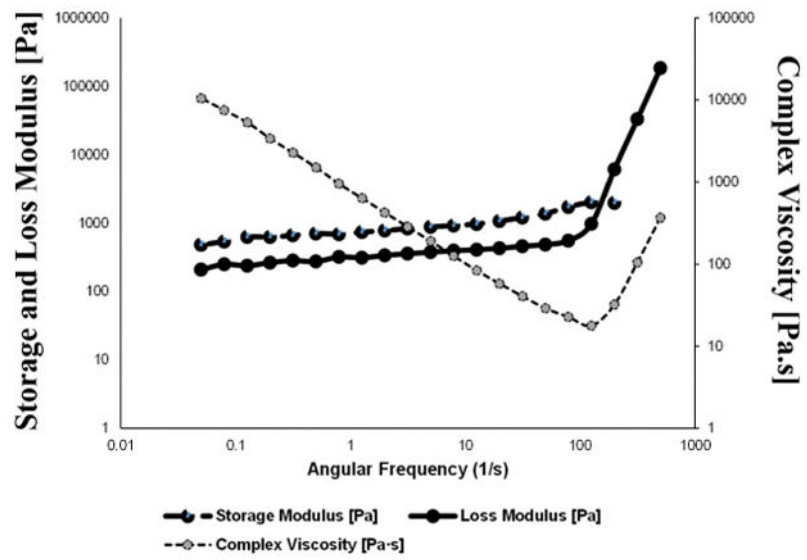
(B) Pre- (left) and post-crosslinked (right) hydrogel (sheet)

(C) Versatility of patterns being printed (ring: left and sheet: right)

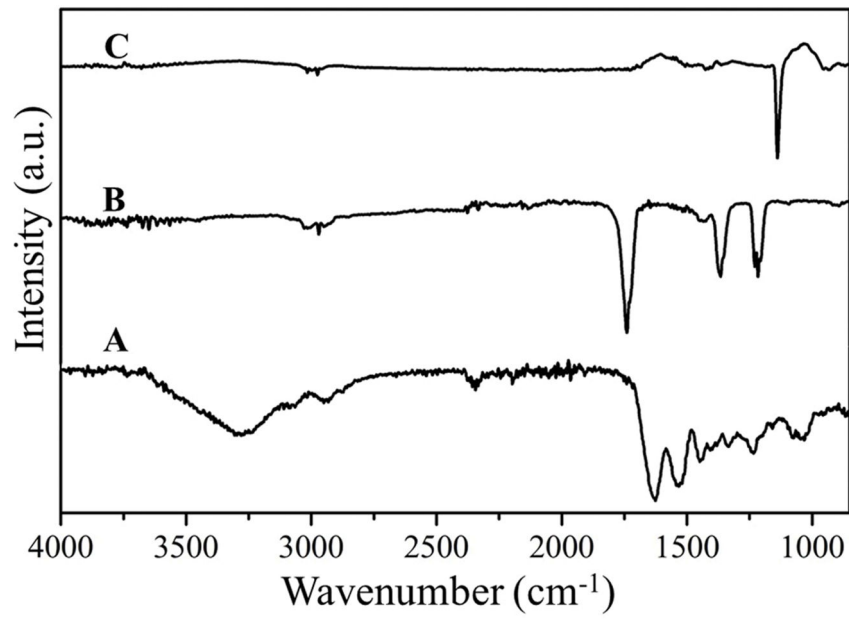
(D) Double layered sheet printing feasibility (en-face: top and cross-section: bottom).

In B, C and D, yellow corresponds to RF and pink to RB being used. Scale bar in all images corresponds to 2 cm.

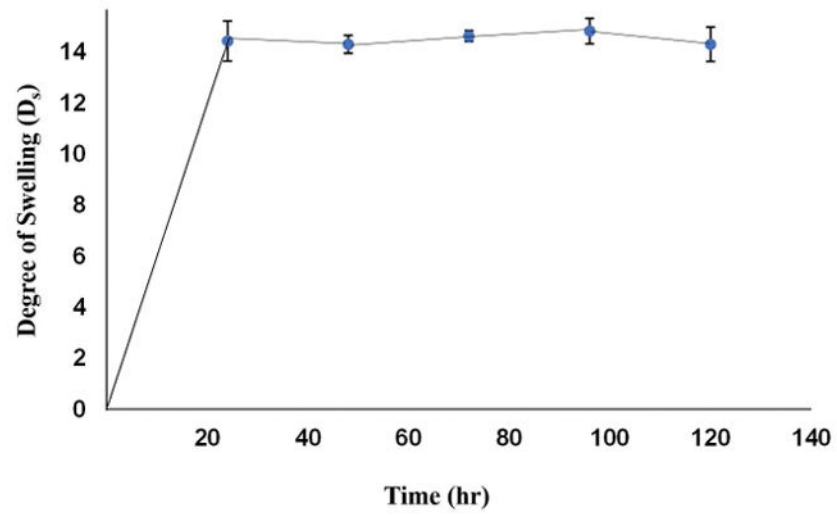




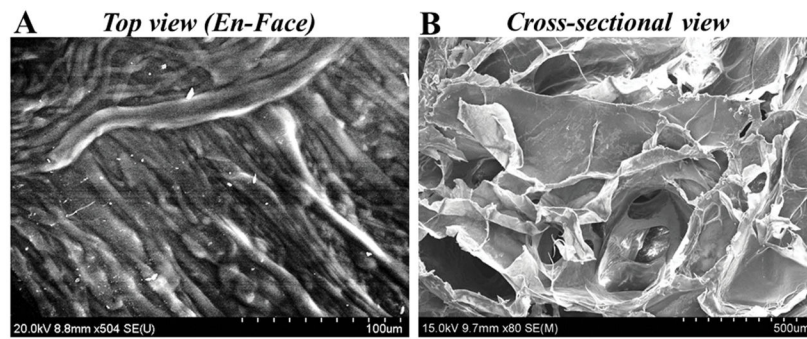
**Figure 2.** Rheology analysis of f-gelatin based hydrogels. Shown is a characteristic dataset obtained from a disc shaped (8 mm) sample of printed crosslinked f-gelatin hydrogel sample.



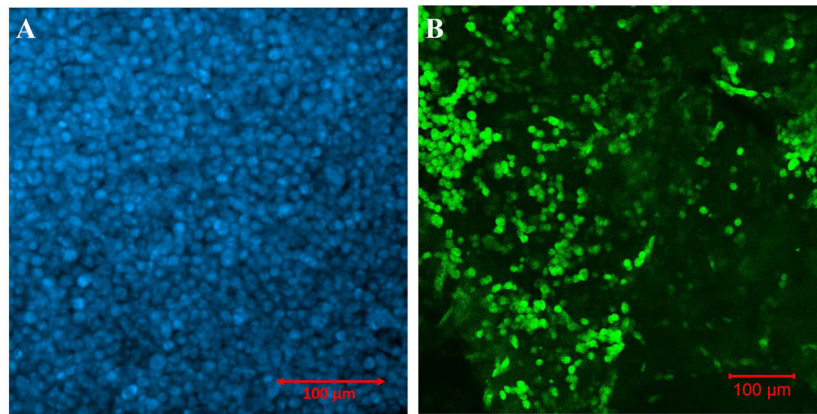
**Figure 3.** (A) FTIR spectrum of crosslinked f-gelatin in the presence of RB and HA. (B) FTIR spectra of f-gelatin and (C) of HA respectively.



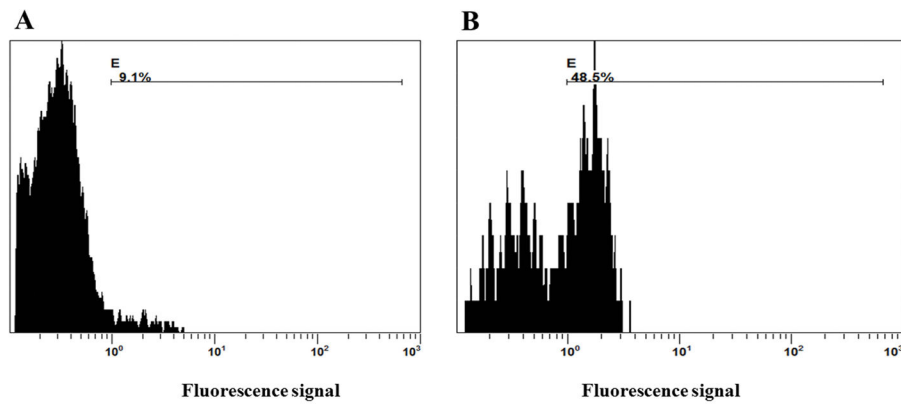
**Figure 4.** Degree of swelling of a printed sheet sample of f-gelatin after crosslinking.



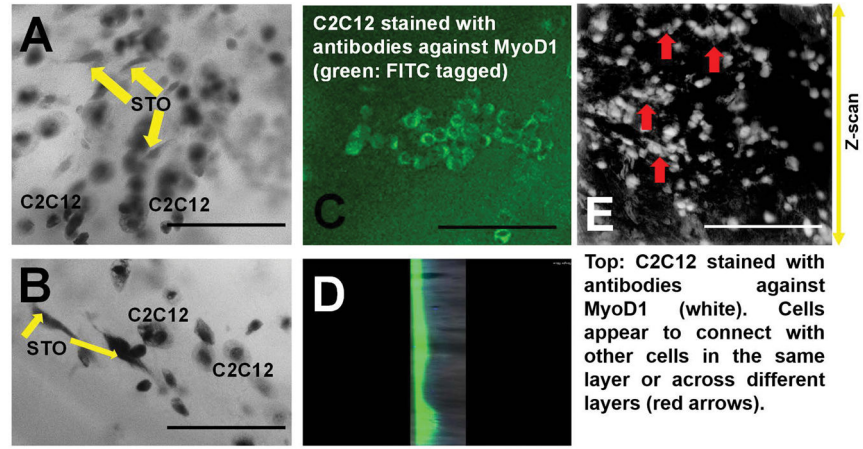
**Figure 5.** Representative image acquired using SEM of a printed sheet sample of f-gelatin after crosslinking.



**Figure 6.** (A) Viability of the mouse MSC stained with Hoechst (blue), post printing after 24 hr. (B) Retention of mouse MSC, pre-stained with PKH67 (green), within the bioprinted construct after 5 days of culture.



**Figure 7.** FACS analysis to show cell proliferation and biocompatibility of the printed sheet structures of f-gelatin after crosslinking. Cells pre-stained with cell trace violet were cultured upto (A) 24 hrs and (B) 72 hrs within printed constructs.


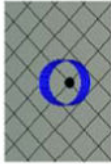


**Figure 8.**

In A and B, shown are bright field z-scans of STO fibroblasts (elongated spindle shaped) co-cultured with C2C12 myoblasts cells (rounded enlarged, confirmed in C and in E). Scale bar is 150  $\mu\text{m}$  in A, B and 200  $\mu\text{m}$  in C and E. In C, a single plane (cross section) was imaged whereas in E, a Z-scan was run spanning several planes as indicated with the arrow (right hand side). In D, shown is a single slice of z-stack section showing top layer (fluorescent: green for C2C12) and bottom layer (non-fluorescent: STO).

**Table 1**

Print settings used to print the rectangular sheet and circular (ring) structures.

Structure	Printing method	Needle diameter (mm)/ Gauge (G)	Extrusion speed (mm/s)	Extruder temperature (°C)	Bed temperature (°C)	Extrusion Pressure (psi)
Rectangular structure* 	Traditional	0.34-0.43/ 23-25	5	Room temperature	Room temperature	4.5±1.9
Circular structure 	Traditional	0.34/ 23	5	Room temperature	Room temperature	2.8

\* The rectangular structure was designed in-house using SOLIDWORKS and the circular structure was obtained from BIOBOTS (design: Bronchi). To print the multilayer rectangular structure using a single print head, we adopted an innovative approach. In this method, the print command was given for more than 2 layers at once. First, the printer was initialized (a petri dish was used as a base/substrate), followed by printing of first layer using material "A" (filled in a syringe). After the printing of the first layer of material "A", printer was stopped and print head was initialized according to the printed structure (considered base/substrate in this case) without changing the position of the printed structure. After this, material for the second layer "B" was loaded in a new syringe. Now, the second layer was printed atop the first layer and after completion, the printer was stopped.